

MODELING AND ANALYSIS METHOD ON CRASHWORTHINESS OF CIVILIAN AIRCRAFT FUSELAGE STRUCTURES

Heyuan Huang, Meiyang Zhao, Wenzhi Wang ,

School of Aeronautics, Northwestern Polytechnical University, Xi'an Shaanxi,
China

Keywords: crashworthiness, finite element model, fuselage, dummy

Abstract

In the paper, numerical simulations of an aircraft fuselage structure with 3-D human body models are performed to study its crashworthiness and passengers' security with the dynamic simulation method. For civilian aircraft fuselage structure with four human body models, finite element model is established and compared with the safety standards to do evaluation for the purpose of improving the aircraft design and occupant's survivability chances in a survival accident. It is found that a reasonable weaknesses setting on the fuselage structure and elastic rebound movement of the fuselage frame are advantageous in the energy absorption during the impact process. Meanwhile, the pelvis load is on the most severe level in all damage data which can be measured by the floor deformation efficiency and reducing occupant's head down and up oscillation frequency is better to decrease the head injury criterion of HIC.

1. Introduction

Safety is the basic requirement for a civil aircraft. In order to improve occupant survivability chances in a survival accident, the load during the crash process for the occupant in the

civil aircraft structure must be suffered in their affordable range. In the crash process, the energy is mainly adsorbed through the fuselage structure and seat system. Therefore, doing deep research on the fuselage structure and seat system performance with dummies is very important to improve the occupant survivability.

Currently, the experiment is the most reliable method to evaluate the aircraft fuselage structure crashworthiness, but various experiments make the design cycle too long and costly trials. However, the numerical simulation method can significantly shorten the design cycle and effectively simulate various crash environments. Therefore, the method of establishing finite element models to develop the simulation analysis program has been the key research content of the aircraft structure crashworthiness simulation.

Soltis [1] analyzed the dynamic performance based on the full-scale aircraft impact test corresponding with standard analysis. Adams [2] confirmed that the finite element model was a new low-cost and effective evaluation method for aircraft seat crashworthiness design. Olschinka [3] used the LS-DYNA software to simulate the dynamic response of the aircraft seat system and concluded that the LS-DYNA was an effective means to

analyze the dynamic response of the aircraft seat system under collision. Gabler [4] established the finite element model using LS-DYNA software with the dummy placed in the aircraft seats and obtained the dummy damage under different impact velocities. Lankarani [5] analyzed a typical seat finite element modeling case and suggested that it was more efficiently using shell element to model dummies than mixed using shell element with solid element.

The paper evaluates the crashworthiness index of a certain aircraft and the passenger impact dynamic response characteristics from the specific view based on the numerical simulation technology. Meanwhile, the crashworthiness of civilian aircraft fuselage structures with dummies is simulated by the finite element analysis software LS-DYNA and compared with impact test results. At last, some design ideas are proposed to improve the passenger seat system crashworthiness performance by comparing the kinds of occupant injury indicators.

2. Dynamical simulation method

2.1 The basic principle of simulation

Crashworthiness analysis is a complex transient physical process which has obvious nonlinear characteristics and needs to use the spatial discretization technique and the discrete time-domain techniques based on the finite difference method of calculating. The commercial software LS-Dyna is used in the paper to solve such problem.

LS-Dyna [6] uses central difference method with time t to calculate the

acceleration a_t :

$$\{a_t\} = [M]^{-1} ([F_t^{ext}] - [F_t^{int}]) \quad (1)$$

Where M is the node quality matrix;

F_t^{ext} is the applying external force and physical force vector; F_t^{int} is the internal force vector which is composed as follow:

$$F_t^{int} = \sum \left\{ \int_{\Omega} B^T \sigma_n d\Omega + F^{hg} \right\} + F^{contact} \quad (2)$$

The three elements in the formula are the equivalent nodal force, the hourglass resistance and the contact force vector of the stress field of the current time unit.

Because the M is a diagonal matrix, the equation can be obtained by a linear equation. The node acceleration is affected by the quality of the node and the resultant force on it. The node speed and its displacement are obtained by the formulas (3) and (4):

$$\{v_{t+t/2}\} = \{v_{t-t/2}\} + \{a_t\}t_t \quad (3)$$

$$\{u_{t+t}\} = \{v_t\} + \{v_{t+t/2}\} \{(t_t + t_{t+t})/2\} \quad (4)$$

2.2 Multi-rigid dynamics of the human body

The human body is a complex organizational structure which is simplified as 5 parts: the head, chest, pelvis, upper body and lower extremity. Lagrange equation is used in the dynamic human body analysis and the inertial coordinate system of all rigid bodies are expressed with B_n [7~8] ($n=1,2,\dots,17$) as $r_n=(x_n,y_n,z_n)^T$ the Euler angle $P_n=(\varphi_n,\theta_n,\psi_n)$ which is rotation of the rigid body coordinates relative to the inertial coordinate system is set as

generalized coordinates, $q_n = (r_n^T, p_n^T)^T$.

Rigid body angular velocity ω_n can be expressed in the formula (5):

$$\omega_n = B_n p_n' \quad (5)$$

The B_n is the coordinate transformation matrix between inertial coordinate system and rigid body reference coordinate system and can be expressed as follow:

$$B_n = \begin{pmatrix} \sin \theta \sin \phi & 0 & \cos \theta \\ \cos \theta \sin \phi & 0 & -\sin \theta \\ \cos \phi & 1 & 0 \end{pmatrix} \quad (6)$$

Rigid body kinetic energy can be expressed as formula (7):

$$T_n = \frac{1}{2} r_n'^T m_n r_n' + \frac{1}{2} \omega_n^T J_n \omega_n \quad (7)$$

Where, r_n' represents physical heart rate, \vec{r}_n is the array matrix in the inertial coordinate system, ω_n is the rigid body angular velocity, $\vec{\omega}_n$ is the array matrix in its own rigid coordinate system, m_n is the rigid mass matrix, J_n is the rigid body inertia tensor, \vec{J}_n is the rotation inertia matrix in its own coordinate system. Submitting the formula (5) into (7) can obtain the kinetic expression Euler angle as follow:

$$T_n = \frac{1}{2} r_n'^T m_n r_n' + \frac{1}{2} p_n'^T B^T J_n B p_n' \quad (8)$$

Lagrange multiplier equation of every rigid element under the generalized coordinates is:

$$\frac{d}{dt} \begin{bmatrix} \left(\frac{\partial T_n}{\partial r_n'} \right)^T \\ \left(\frac{\partial T_n}{\partial p_n'} \right)^T \end{bmatrix} - \begin{bmatrix} \left(\frac{\partial T_n}{\partial r_n} \right)^T \\ \left(\frac{\partial T_n}{\partial p_n} \right)^T \end{bmatrix} + \begin{bmatrix} \Phi_{r_n}^T \lambda \\ \Phi_{p_n}^T \lambda \end{bmatrix} = \begin{bmatrix} Q_{r_n} \\ Q_{p_n} \end{bmatrix}$$

(9)

Where, λ is the Lagrange multipliers, $\Phi_{r_n}^T$ and $\Phi_{p_n}^T$ respectively represents the partial derivative solution of constraint equations under the generalized coordinates.

The rigid body motion equations are combined together and obtain the unified dynamic equation as formula (10):

$$\begin{cases} Mr'' + \Phi_r^T \lambda - Q_r = 0 \\ \Gamma' - \frac{\partial T}{\partial p} + \Phi_p^T \lambda - Q_p = 0 \\ \Gamma - B^T J B p' = 0 \end{cases} \quad (10)$$

3. Finite element models details

3.1 Finite element model of aircraft fuselage structure

Firstly, the 3-D digital model established in Catia is imported into HyperMesh to be meshed and generated the K file. Then, the K file is submitted to LS-Dyna solver and output acceleration curves and speed curves. The process is shown in the Fig.1.

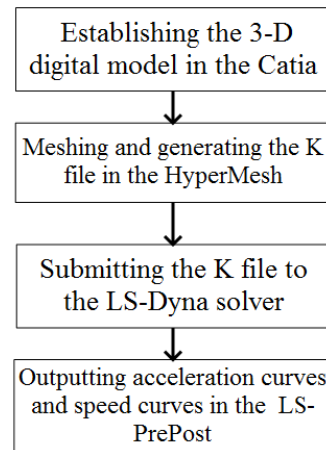


Fig.1 The flowchart of modeling and calculation

A certain type of aircraft which is made in China is taken as the study object which contains 7 parts: skin, body

frame, purlin, columns, floor beams, rails and centralized mass in the finite element model. The finite element

models of all the components are shown in the Fig.2.

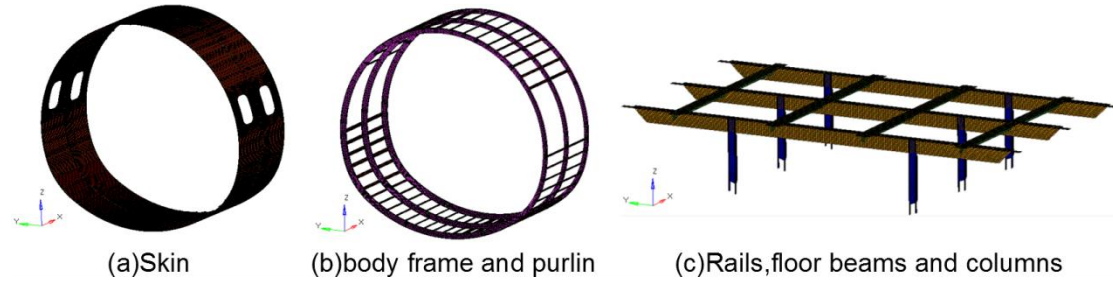


Fig.2 Finite element models of the aircraft fuselage structure

The Al-2024-T3, Al-7075-T6 and Al-7150-T77511 are used in the fuselage section with the bilinear elastic-plastic constitutive model and strain failure criterion. Material mechanical properties are shown in the table.1.

and skin is surface to surface contact, between fuselage frame and ground is node to surface contact, the dynamic friction factor of both contacts is 0.1 and the static friction factor is 0.2. The impact velocity is 7.0m/s.

The contact type between ground

Table.1 Mechanical properties of the fuselage structure

Material	Al-2024-T3	Al-7075-T6	Al-7150-T77511
Parts	Skin	Fuselage frame& Stringers	Column& Floor beam
Elastic Modulus	66.3	71.0	72
Poisson's ratio	0.33	0.33	0.36
Density	2796	2768	2832
Yield modulus	243	362	538
Strengthening modulus	826	1001	679
Failure strain	0.14	0.045	0.07

3.2 Finite element model of seating system and occupants

3.2.1 Simplified model of the seating system

The seat and its cushion are simplified as two planes with the angle of 100°. The tripod and seat legs are truss element with radius of 25mm; the aircraft fuselage frame is approximately to be a circle of 2.6m in diameter and the floor width is about 2.3m, the cabin channel width is 0.4m, the gap between neighboring seats is 0.1m. The aircraft seat arrangement is shown in the Fig.3.

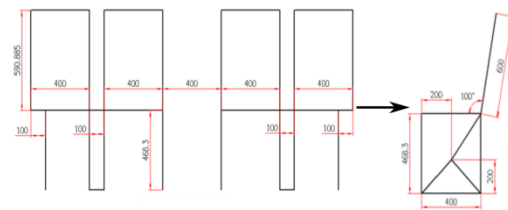


Fig.3 Seats arrangement and size parameters

3.2.2 Finite element model of occupants and seat safety belt system

The LSTC Hybrid III 50th Rigid-FE dummy model is used in the simulation to replace the occupant which has 50% of the normal adult male body and is shown in the Fig.4-(a). The contact force penetration curve which is shown in the

Fig.4-(b) is employed to simulate the dummy and seat cushion contact force.

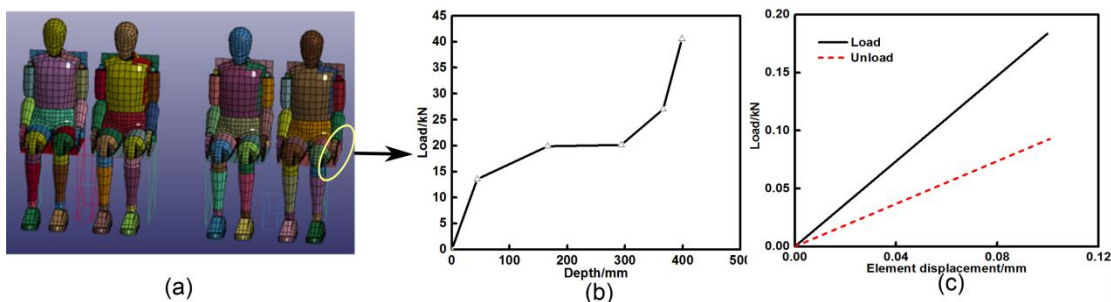


Fig.4 The dummy models: (a) dummy location map ;(b) contact force penetration curve;(c) The load-unload displacement relationship curves

The security belt is set in the LS-PREPOST. The length of 1-D beam element is 94mm with the Belytschko-Tsay membrane element; the Ribbon cell size of 2-D element is 11.75mm and 1.2mm in thickness. The corresponding load-unload displacement relationship curves are shown in the Fig.4-(c).

3.3 Model of full-size aircraft fuselage structure with four dummies

The quality of the seat system is 352kg and the quality of fuselage structure is 84.7kg. The seat legs and the floor are used to connect by the node merging and the details of seat system connection are shown in the Fig.5.

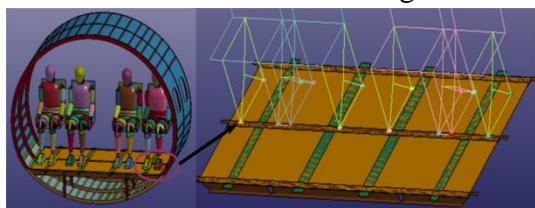


Fig.5 The detail of the seat system

4. Result and discussion

4.1 The aircraft fuselage structure crashworthiness

The Fig.6 is the deformation and strain diagram of the aircraft fuselage structure. It can be seen that the crash process can typically be divided into two stages: the first one is the fuselage

touchdown phase, which appears damage at the bottom of the fuselage frame section and accompanies with the first acceleration peak; the second one is the concentrated failure stage that destruction extends from the fuselage frame bottom to the cabin support connections. In this impact process, the cabin support occurs bending but it is no longer extends to both sides, at the same time, the load transfers to the cabin and results in the second acceleration peak.

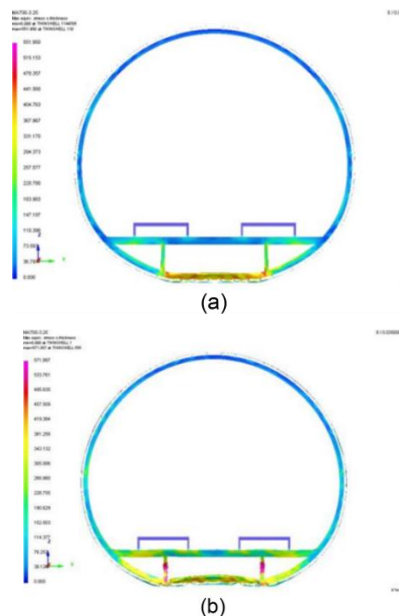


Fig.6 The deformation and strain diagram of the aircraft fuselage structure: (a)t=0.02s;(b)t=0.035s

The Fig.7 is the acceleration history curve for 4 reference points which are set in the seat to observe the change of

seat acceleration when the occupant is impacted on the cabin. All the acceleration curves appears a peak about 18g in 20ms, which is corresponding to the first stage of crash scenarios; the second stage is about 280ms to 580ms and appears the second peak on 340ms. The maximum peak value of four reference points is 42.6g and the minimum is 31.8g. Start from 500ms, all curves are not increasing and the acceleration curves also decrease rapidly. Because the support plate is close with the bottom plate, in a very short time after the floor deforms, the bottom plate begins to damage. Therefore, there is almost no extra time from the first phase of deformation to enter the second stage of the deformation.

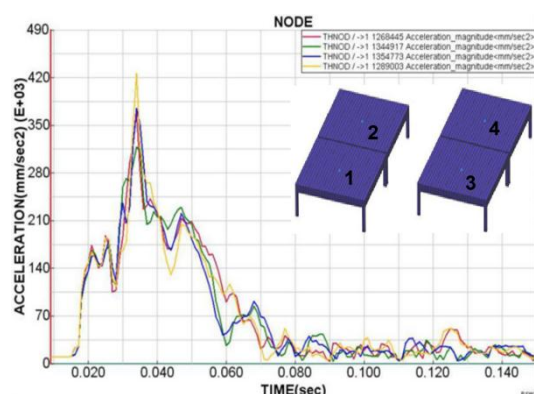
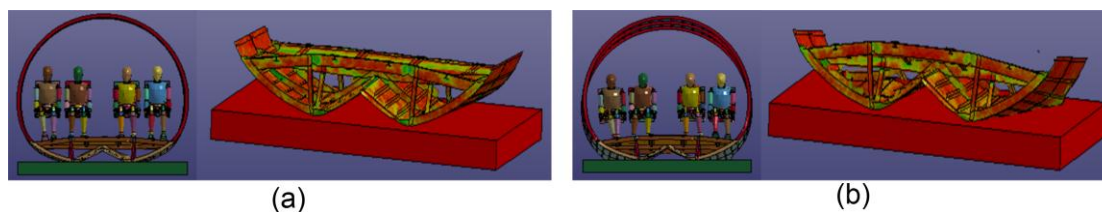


Fig.7 The acceleration curves for 4 reference points on the seat

movement situation from 0 to 200ms during the crash scenarios. The dummies are numbered I、II、III、IV from left to right and fuselage frames are numbered I、II、III from front to back. It can be seen that bottom frame II and III and skin appear war-page on the 50ms time and touch to the beam and floor. Four pillars under both frames have been fracture instability and the floor is suffered larger force. From 100ms to 200ms, the deformation of frames and skin decrease and there is a restitution movement trend. During the whole process of simulation, both frames and skin are not off the ground. Before 50ms time, the frames structural deformation offered dummies sufficient energy absorption, so the interaction between dummies and the seat cushions are not very obvious. During 50ms to 100ms periods, dummies have shown bow down movement but their legs are not apparent action. From 100ms to 200ms, there is frame structural segment rebound deformation and the middle floor is jacked up. So four dummies' legs swing to the both sides of the fuselage frame respectively and only dummy IV's left leg appears the kick action.

4.2 Dummies' survivability analysis

The Fig.8 is about aircraft fuselage deformation and four dummies



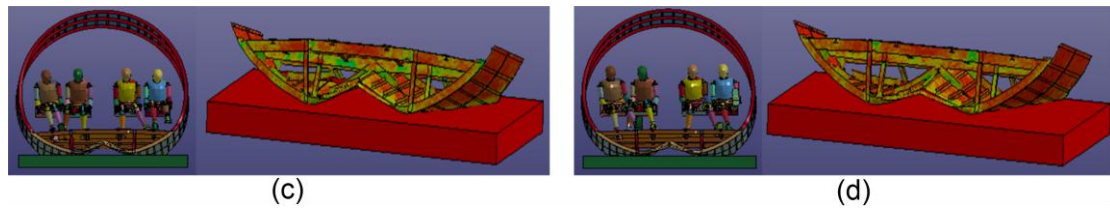


Fig.8 The damage and deformation of dummies and the aircraft fuselage structure: (a)50ms; (b) 100ms; (c) 150ms; (d) 200ms

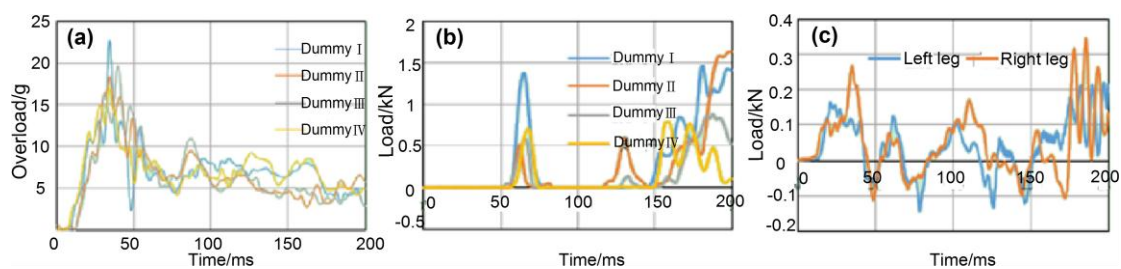
The Fig.9 is the dummies' injury data during the crash. It is known according to the Fig.9-(a) that the maximum head overload of four dummies respectively appeared at time 34ms, 34ms, 40ms, 34ms and peak overload are 22.6g, 18.3g, 19.7g and 16.9g. After 34ms, all the dummies' head overload rapidly decay to 5g. By calculating with formula HIC [9~10], their HIC are 16.03, 19.76, 22.16 and 16.02. The peak overload of dummy I is the largest but the waveform is sharp and short duration, therefore the HIC value is not very high. Following the crash process, there is a huge deformation on the aircraft fuselage frame to absorb impact energy which results in dummy head overload rapidly decreasing.

Fig.9-(b) reflects belt restraint loads. All curves express two peaks at 70ms and 200ms. The load reaches the maximum value on 200ms and respectively is 1466.7N, 1641.1N, 877N and 787N.

Fig.9-(c) to Fig.9-(f) is about four dummies' thigh femurs axial compression overload. It is known the left thigh femur compression load

maintains the highest level from 150ms to 180ms and their femur maximum compression load are 344.4N, 549.7N, 278.6N and 702.8N. In conjunction with Fig.6, the dummy IV has a significant movement to lift its left leg off the floor and reaches the maximum position in 200ms. Under the effect of centrifugal force, the femurs endure a huge overload. Since the restriction on feet and legs by the floor, other three dummies only have slight swing movement, so their thigh femur maximum compressive overload is smaller than the dummy IV.

Fig.9-(g) is the dummies' pelvic compression load curve. In time vicinity to 38ms, all curves reach the peak. Combining with the Fig.6, it can be known from 0ms to 50ms, dummies strongly act on the seat cushion and the pelvis plays a crucial role in this contact and bears the load which is also larger than any other time. Due to structural deformation has an important role in the buffer for dummies and box and skin warping ease the mutual compression effect between dummy buttock and cushion, both of them relieve the dummies' pelvis overload.



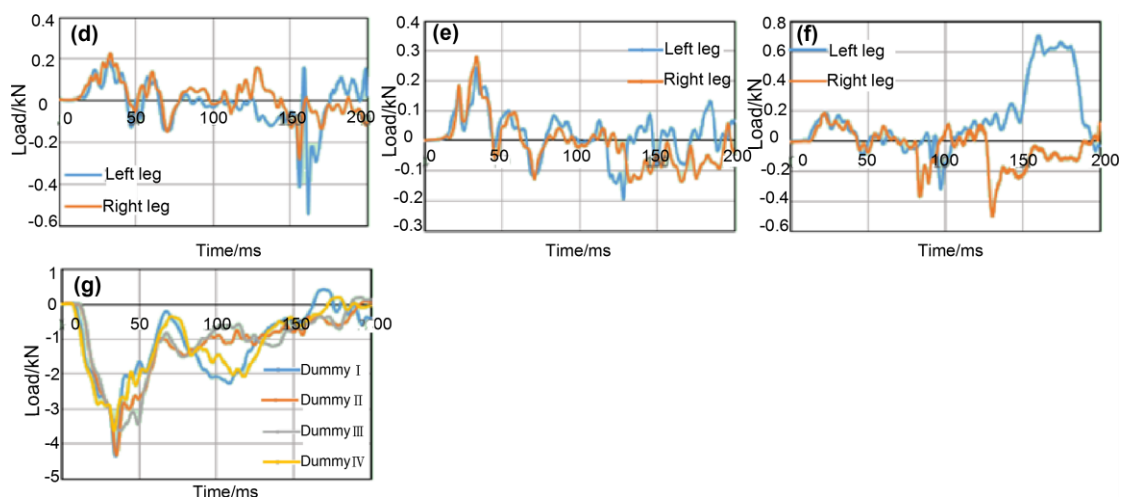


Fig.9 The dummies' injury data:(a) head overload;(b) belt restraint loads;(c)~(f) thigh femurs axial compression overload of dummy 1to 4;(f) pelvic compression load

The respective peak data in the Fig.9 is included in the Table.2 and gets occupant damage assessment combined with related evaluation criteria on the crashworthiness airworthiness regulations. It can obviously be seen in the table that seat belt load, femur compressive load, HIC and pelvic compression load meet the airworthiness

requirements and the maximum results by simulation have a certain margin distance with airworthiness requirements. In concluded, the aircraft fuselage structure with four dummies meets the crashworthiness airworthiness regulations at the crash conditions with 7m/s hitting rate.

Table.2 Evaluation of passengers' injure

Max load (N)	Airworthiness Requirements	Max values of simulation				Evaluation result
		Dummy 1	Dummy 2	Dummy 3	Dummy 4	
Safety belt	<7784	2262.7	1181.5	953.1	1516.5	Achieved
Pelvis	<6672	6052	6104.8	5653.6	6263	Achieved
Leg	<10008	542.6	757	540.7	1170.8	Achieved
HIC	<1000	38.54	46.85	40.39	38.45	Achieved

5. Conclusions

In this paper, according to the appropriate civil aircraft airworthiness regulations, the crashworthiness performance of an aircraft fuselage structure with four passengers is evaluated by numerical simulations and gets following conclusions:

1. In order to improve the aircraft fuselage structure crashworthiness, the space under the cabin floor should deform as much as possible so that more materials can be involved in the energy

absorption process.

2. The passenger's head overload mainly depends on the pre-contact when the fuselage structure contacts with the ground and bow action, the fuselage overall shock rebound movement will have buffer action to the head. Meanwhile, reducing the elastic rebound movement of the fuselage frame is beneficial to reduce the corresponding safety belt restraint load.

3. In the process of crash, it is better to reduce the occupant's head down and up oscillation frequency

which means the lower of head movement amplitude and frequency, the smaller of head injury criterion (HIC).

4. The pelvis load is on the most severe level in all damage data. The floor deformation efficiency is a very important indicator to measure the pelvis load. The faster and greater of floor deformation, the smaller of the corresponding seat cushion to the occupant hips and thighs back force and the smaller load pelvis.

References

- [1] Soltis.S.J., Nissley W.J.. The development of dynamic performance standards for civil aircrafts seats[J]. Society of Auto motive Engineers, 1985,(3):118-134.
- [2] Adams A , Lankarani HM ,A modern aerospace modeling approach for evaluation of aircraft fuselage crashworthiness[J]. International Journal of Crashworth- iness, 2003, 8(4):401-413.
- [3] Olschinka C., Schumacher A. Dynamic Simulation of flight passenger seats[R]. Japan: 5th LS-Dyna conference, 2006:25-34.
- [4] Gabler H., Bowen D., Molnar C. Modeling of Commuter category aircraft seat [R]. U.S.: Department of Transportation, 2004:47-66.
- [5] Lankarni H., Bhone P. Finite element modeling strategies for dynamic aircraft seats [J]. Society of Automotive Engineers, 2008, (1):98-112.
- [6] Anon., LS-DYNA3D User's Manual, Livermore Software Technology Company, Livermore [Z], CA, 1997.
- [7] LIULEI. Modeling Methods for Simulation of Human Motion [J]. Computer Simulation, 2009,(1):79-86.
- [8] QIN Rui-rui.Virtual Simulation of Human Walking Based on Multi-rigid-body Dynamics Model [J]. Research and exploration in laboratory, 2012, (6):149-168.
- [9] Federal Aviation Administration. Advisory Circular 25.562-1B. Dynamic Evaluation Of Seat,Restraint Systems and Occupant Protection on Transport Airlines[Z]. 2006.
- [10] SAE Aerospace Standards AS8049B. Performance Standard for Seats in Civil Rotorcraft,Transport Aircraft and General Aviation Aircraft[Z]. 2005.

Copyright Statement

The authors confirm that they and their company or organization, hold copyright on all of the original material included in this paper. The authors also confirm that they have obtained permission, from the copyright holder of any third party material included in this paper, to publish it as part of their paper. The authors confirm that they give permission, or have obtained permission from the copyright holder of this paper, for the publication and distribution of this paper as part of the ICAS proceedings or as individual off-prints from the proceedings.

Contact Author Email Address

Contact Author:HEYUAN HUANG

Email Address:

npuhhy@mail.nwpu.edu.cn